Nanochem Res 2(2): 248-260, Summer and Autumn 2017

REVIEW PAPER

All Procedures for the Synthesis of Silver Nanosheets

Zarin Moghadam[1], Kamran Akhbari[1,*], Fahimeh Jamali[2], Fatemeh Shahangi Shirazi[1]

[1] *School of Chemistry, College of Science, University of Tehran, Tehran, Iran*

[2] *Department of Chemistry, Payame Noor University (Abhar centre), Zanjan, Iran*

ARTICLE INFO

Article History:
Received 28 April 2017
Accepted 13 June 2017
Published 1 July 2017

Keywords:
Calcination
Coating Technique
Deposition
Mirror Reaction
Redox Reaction
Silver Nanosheets

ABSTRACT

Two dimensional silver(I) coordination polymer, $[Ag(\mu_5\text{-T4S})]_n$ (1), ($T4S^-$ = toluene-4-sulfonate), has been synthesized and characterized by Inductively Coupled Plasma (ICP) and elemental analyses, IR spectroscopy and powder X-ray diffraction. This compound was calcined at 450, 500 and 700 °C in a furnace and static atmosphere of air. The resulting compound from 1 at 450 °C is a spongy nanostructure which could not be characterized due to its partial calcination process .At 500 and 700 °C, the compound is a mixture of silver and silver sulfate compacted nanosheets and microstructures. By increasing the temperature from 500 to 700 °C, the tendency for the formation of agglomerated mixture of silver and silver sulfate was increased. In addition, a number of one-step techniques including electrochemical deposition method, electroless deposition method, direct deposition method, redox reaction, mirror reaction, coating technique, self-seeding or self-assembling process and wet chemical method have been reviewed for the synthesis of two-dimensional nano silver.

How to cite this article
Moghadam Z, Akhbari K, Jamali F, Shahangi Shirazi F. All Procedures for the Synthesis of Silver Nanosheets. Nanochem Res, 2017; 2(2):248-260. DOI: 10.22036/ncr.2017.02.012

INTRODUCTION

In recent years, nanostructured materials have been considered for their new properties such as magnetic, electronic, catalysis and optical which cannot be observed in their bulk form. [1] For instance, because of high surface area and dipole-dipole interaction of magnetic nanoparticles, [2] they have drawn enormous attention over their potential use in biomedical applications. [3] For example, ferrite nanostructures, a special branch of ferromagnetic material, have received special attention due to their good magnetic and high electrical properties [4]. Furthermore, some inorganic nanoparticles coated with organic layers could function like globular proteins [5]. Also, the higher stability and lower cost of nanoparticles compared with proteins, as very interesting features, have attracted the researchers' attention in the artificial design of enzymes [5,6]. Coordination polymers are infinite systems built up with metal ions and organic ligands as main elementary units linked via coordinative and other weak chemical bonds [7-9]. Among polymeric coinage d^{10} metal complexes, silver(I) coordination polymers have received much attention because silver(I) shows a tendency to form coordination polymers with unique Ag-C and Ag-Ag interactions [10-17]. In the past decade, several coordination polymer networks of Ag^+ have been synthesized and investigated. Like gold, silver is a rare metal and holds great value and is also traded in similar markets. It is also used in the manufacturing of batteries as well as a catalyst. Silver has also played a vital role in photography and, consequently, in medicine. Metal nanostructures have received considerable attention in both scientific and technological areas due to their unique and unusual physico-chemical properties compared with bulk

* Corresponding Author Email: *akhbari.k@khayam.ut.ac.ir*

materials [18]. They have been the focus of intensive research in the past several decades due to their potential application in conductive electrodes and in optical, optoelectronic, and magnetic devices [19]. Nowadays, many research activities have been performed on silver nanoparticles because of their important scientific and technological applications in color filters [20], optical switching [21], optical sensors [22], and especially in surface-enhanced Raman scattering [23-25]. Also, silver nanostructures of different shapes, such as cubes and octahedrons tetrahedrons, wires/rods and plates/sheets have attracted high research interest, due to their unique and tunable optical properties, as well as their wide potential applications, such as optical probes, optical labels, chemical and biological sensors. Among them, two-dimensional (2-D) silver nanosheets have specially attracted attention in the past decade, including triangular plates/sheets, nanodisc, and hexagonal plates [26]. Continuing to our previous works on using coordination polymers as new precursors for preparation of silver nanostructures [27-32], in this work, we use $[Ag(\mu_5\text{-T4S})]_n$ (**1**), ($T4S^-$ = toluene-4-sulfonate) as new precursor for preparation of nano silver. Also, the effect of thermolysis temperature on formation of attributed nanostructures is investigated. In addition, the work presented herein supplements all synthetic procedures for preparation of silver nanosheets.

EXPERIMENTALS

Materials and Physical Techniques

All reagents and solvents for the synthesis and analysis were commercially available and were used as received. The plots of molecular structures were prepared using Mercury. Microanalyses were carried out using a Heraeus CHN-O- Rapid analyzer. The amounts of metal ions in each sample were measured by Inductively Coupled Plasma (ICP) analyses. Melting points were measured using an Electrothermal 9100 apparatus and are uncorrected. IR spectra were recorded using an Equinox 55 FT-IR spectrometer (Bruker, Bremen, Germany) in the ATR form, in the range of 400-4000 cm^{-1} with a 4.0 cm^{-1} resolution and 16 scans. X-ray powder diffraction (XRD) measurements were performed using an X'pert diffractometer manufactured by Philips with monochromatized Cukα radiation (λ = 1.54056 Å) with a step size of 0.01671 (degree). The X-ray source was operated under a voltage of 40 kV and a current of 30 mA. Bragg-Brentano was used as the source detector geometry with a scintillation detector. Additional attachments or peripheral equipment, such as an anti-scatter slit (1°), divergence slit (1°), monochromator and soller slit (0.04 rad) were also used in this diffractometer. The samples were prepared as fine powders on silicon based material. Simulated XRD powder patterns based on single crystal data were prepared using the Mercury software. The samples were characterized with a scanning electron microscope (Philips XL 30) with a gold coating.

Synthesis of $[Ag(\mu_5\text{-T4S})]_n$ (1) and preparation of its nano silver

In 30 mL acetonitrile 1.720 g (10 mmol) toluene-4-sulfonic acid (HT4S) was added and stirred with a solution of 0.570 g (10 mmol) KOH in 5 ml H_2O to form a clear solution. Addition of 1.690 g (10 mmol) $Ag(NO_3)$ in 5 ml H_2O produced a clear solution that was stirred and then allowed to stand in darkness at room temperature to evaporate for several days to obtain pure single crystals. The crystals were washed with acetone and air dried, m.p. = 251 °C, Yield: 1.616 g (58%). IR (selected bands; in cm^{-1}): 534m, 560s, 685s, 804s, 842w, 945w, 1000s, 1035s, 1126vs, 1190vs, 1399w, 1439w, and 1487w. Anal. calc. for $C_7H_7AgO_3S$: C, 30.10; H, 2.51; Ag, 38.34%; found; C, 30.25; H, 2.61; Ag, 38.50%. In order to prepare of silver nano-structures, calcination of **1,** as a very thin film, were done at 450, 500 and 700 °C in a furnace and static atmosphere of air for 3 hours.

RESULT AND DISCUSSION

Calcination process

The reaction between toluene-4-sulfonate ($T4S^-$) and $AgNO_3$ led to a crystalline material with a general formula $[Ag(\mu_5\text{-T4S})]_n$ (**1**) [13]. The structure of 1 was determined by X–ray crystallography (Figure 1a) [13]. A Comparison between the XRD patterns simulated from single crystal X-ray data of 1 (Figure 2a) and the prepared sample (Figure 2b), approved the formation of 1 successfully. The structure of compound 1 may be considered as a coordination polymer consisting of two-dimensional sheets constructed from Ag(I) ions and bridging sulfonate groups, running parallel to the *bc* sheet and the individual polymeric layers are almost parallel to each other along a axis, resulting in two-dimensional sheets as shown in Figure 1b. The silver atoms in 1 have $O_5Ag\cdots C$

coordination sphere [13].

In order to obtain silver nanostructures, calcination of 1 powder were done at 450, 500 and 700 °C in static atmosphere of air. Figures 2c-e show the XRD patterns of the resulting compounds prepared by this process, respectively. Figure 2c, which is the XRD pattern residue obtained from calcination of 1 at 450 °C, is different from that of two other samples prepared by calcination of 1 at 500 and 700 °C. The XRD pattern in Figure 2c could not be characterized due to partial calcination process of 1. Two other XRD patterns (Figures 2d,e) are in agreement with the standard patterns of cubic silver (with the lattice parameters a = 4.0862

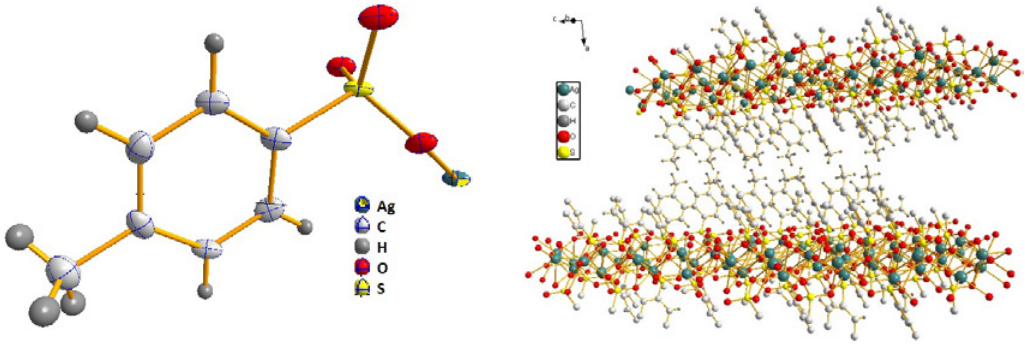

Fig. 1: a) Primary structural building unit of $[Ag(\mu_5\text{-}T4S)]_n$ (1), b) a fragment of the two parallel sheets in compound 1.

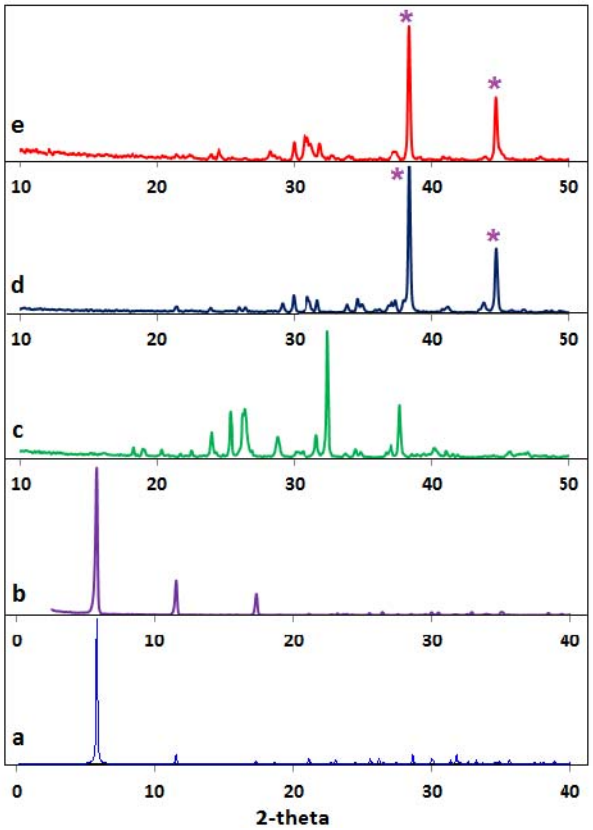

Fig. 2: XRD patterns; a) simulated pattern based on single crystal data of compound $[Ag(\mu_5\text{-}T4S)]_n$ (1), b) crystals of compound 1, c) unknown spongy nanostructure fabricated from calcination of compound 1 at 450 °C, d) packed nanosheets of silver and silver sulfate mixture prepared from calcination of compound 1 at 500 °C, and e) mixture of silver and silver sulfate microstructure prepared from calcination of compound 1 at 700 °C (assigned peaks with star mark are attributed to metallic silver, and other peaks are attributed to silver sulfate).

Å and z = 4 which are close to the reported values JCPDS card number 04-0783) and orthorhombic silver sulfate (with the lattice parameters a = 5.796(3) Å, b = 12.667(7) Å, c = 10.2238(5) Å and z = 8 which are close to the reported values JCPDS card number 80-1270). Considering the TG analysis, we can find the reason of this difference [13]. At 450 °C, the calcination process of 1 is not complete and we could not characterize the residue formed by calcination at this temperature. On the other hand, calcination process of 1 at 500 and 700 °C, resulted in formation of a mixture of silver and silver sulfate nanosheets. Figure 3a shows the SEM image of spongy structure obtained from calcination of 1 at 450 °C. As it is obvious, this spongy structure consists of nanoparticles too (Figure 3b). Figures 3c,d show the SEM images of silver and silver sulfate mixture which obtained from calcination of 1 at 500 °C. The morphology of this compound indicates the formation of silver and silver sulfate mixture nanosheets which were compacted to each other. The effect of calcination temperature increase on the formation of silver and silver sulfate mixture can be observed in Figures 3e,f. It seems that by increasing the temperature from 500 to 700 °C, the tendency of silver and silver sulfate mixture nanosheets for agglomeration is increased and finally the silver and silver sulfate mixture microstructures are formed. Thus, the appropriate temperature of preparation mixture of silver and silver sulfate nanosheets from 1 is 500 °C.

Electrochemical deposition method

High reproducible electro-deposition method was reported by Xia et al. to fabricate silver nanosheets on coper plate with sub-10nm nanogap.

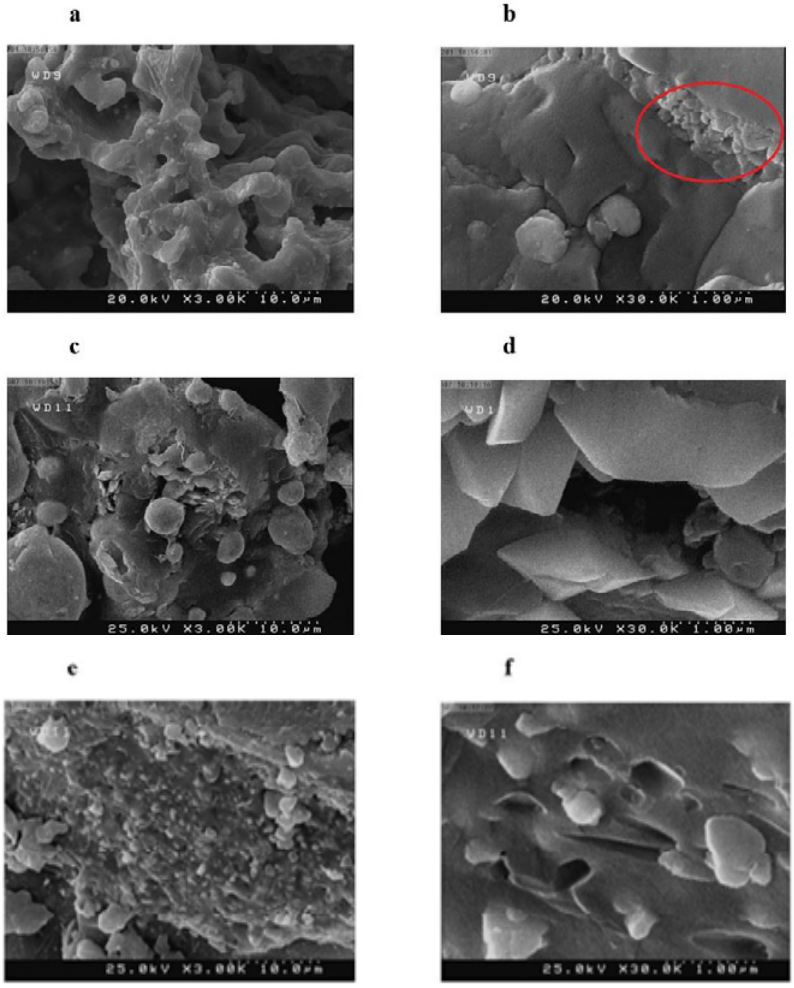

Fig. 3: SEM images of a,b) unknown spongy nanostructure fabricated from calcination of compound 1 at 450 °C, c,d) packed nanosheets of silver and silver sulfate mixture prepared from calcination of compound 1 at 500 °C, and e,f) mixture of silver and silver sulfate microstructure prepared from calcination of compound 1 at 700 °C.

[33] It is a simple and environmentally friendly method. When the copper plate was immersed into the plating solution for 5 min, the 300 nm disordered silver nanosheets were deposited on the copper surface. After 15 min's deposition, the nanosheets became denser. The density of silver nanosheets became higher with the increase of deposition time. When the current density increased, the silver nanosheets grew denser and longer because of the reduction reaction of Ag^{+}. Boric acid acted as the capping agent on the surface of silver nanosheets, and directed the silver in growing along the surface of the sheets [33]. This electro-deposited silver nanosheets can provide effective and reproducible SERS signalswhich have the potential to be widely used in different fields. This method has proved to be applicable on different metal substrates, and exhibited the potential to be widely used in different fields. In this method, the size of the nanogaps can be varied from around 7 nm to 150 nm by adjusting the deposition time and current density.

In another work, synthesis of Ag nanosheets via a facile, one-step, template-free electrochemical deposition in an ultra-dilute silver nitrate aqueous electrolyte is studied. This process uses a template and surfactant-free electrochemical deposition on an ultra-dilute electrolyte of low electrical conductivity. Figure 4 shows the typical SEM images of Ag nanosheets electrodeposited on an ultra-dilute electrolyte in the potentiodynamic mode (VR = 15 V, VO = 0.2 V,100 Hz, and 3%) for 120 min. Ag nanosheets had a width up to approximately 10 µm and a thickness of approximately 30 nm and were grown on the facetted Ag nanowires.

In comparison, when the $AgNO_3$ concentration was 0.2 mM, the facetted granular Ag islands grew with the size of 0.2 to 2 µm, as shown in Figure 5a. With the further increase of $AgNO_3$ concentration up to 2 mM, the granular islands were densely generated and formed a granular (columnar) layer, as shown in Figure 5b. This indicates that the growth of facetted nanowires and nanosheets shown in Figure 4 was closely related to the dilute concentration. The thickness of the nanosheet dependeds on the thickness of the facetted nanowires that grew over the islands

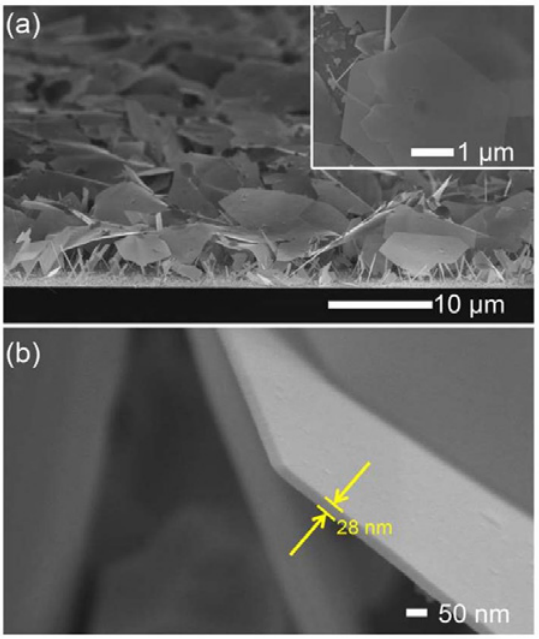

Fig. 4: Typical SEM images of Ag nanosheets. (a) Typical 13°-tilted SEM images of Ag nanosheets grown on a substrate and (b) a higher magnified SEM image of a Ag nanosheet. (The inset indicates a higher magnified top-view SEM image). Reproduced with permission from ref. 34, copyright 2013, Springer.

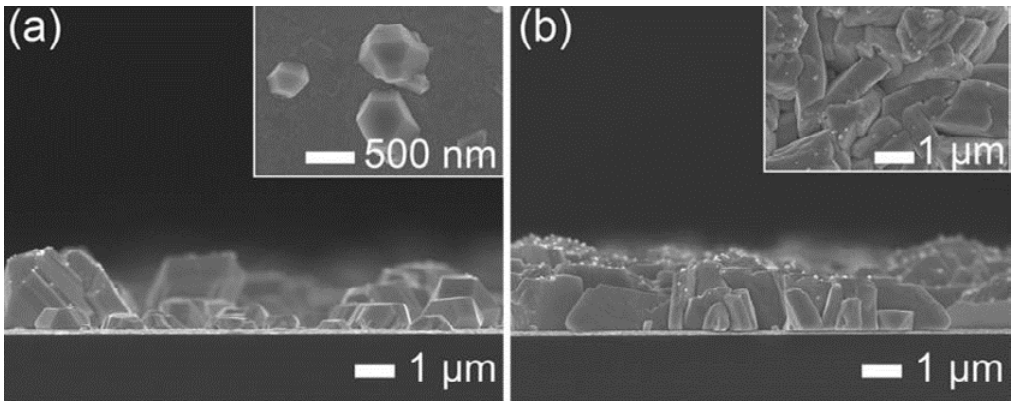

Fig. 5: Typical SEM images of Ag deposits with $AgNO_3$ concentration. Cross-sectional SEM images of Ag deposits deposited in the electrolytes of (a) 0.2 and (b) 2 mM $AgNO_3$ for 120 min (VR = 15 V, VO = 0.2 V, µ0 Hz, and 3%), (The insets denote the top-view SEM images). Reproduced with permission from ref. 34, copyright 2013, Springer.

nucleated on the substrate. Therefore, the thickness of Ag nanosheets could be controlled by varying the island size. In this method, the growth of nanosheets occurred in three stages: polygonal island formation, facetted nanowire growth, and planar growth of nanosheet coherent with the facetted nanowire [34].

Electroless deposition method

Most electroless plating methods are autocatalytic redox processes that involve deposition without any costly equipment in which the driving force for the reduction of metal ions is supplied by a chemical reducing agent in solution. The plating process technique has many advantages for the deposition of metal nanoparticle films, such as low temperature, simplicity, low cost, etc. Recently, Yi et al. reported synthesizing Ag thin films deposited on glass slide substrates at room temperature by the electroless plating technique [35]. The procedure for the in-situ fabrication of Ag nanosheets on quartz glass substrates is shown in Figure 6. In synthesizing solution, Sn^{2+} is absorbed onto the surface of the substrates by the negatively charged ions on the dielectric substrates through electrostatic attraction, then the redox reaction is carried out. In this reaction, Sn^{2+} is oxidized from the bivalent state to the quaternary state, and Ag^{+} is reduced to Ag at the same time. Then, the surface of the quartz glass substrates is covered uniformly with Ag seeds. It was found that the molar ratio of $AgNO_3$ to TEA, the concentration of $AgNO_3$ and the appropriate reaction temperature were the key to in-situ growth of Ag nanosheets on quartz glass substrates [35]. Also, Zhao et al. reported the fabrication of assemblies of silver nanoparticles organized on the microporous walls of the TiO_2 inverse opal film via electroless deposition method. The amount of Ag nanoparticles can be effectively controlled by changing the cycle times. The application of these Ag nanoparticles decorated TiO_2 inverse opal film as SERS substrate are investigated by using R6G as a probe molecule [36].

Direct deposition method

Silver nanosheets can be also generated by direct deposition method such as direct deposition of the silver onto an aluminum foil. Figure 7 shows the SEM images of the oriented 2D silver nanosheets grown on a flat aluminum foil. As can be seen from this figure, the substrate is fully covered with the silver nanosheets. Most of the nanosheets stand on the Al foil with their planes perpendicular to the surface of the substrate, and their sizes range from hundreds of nanometers to several micrometers. Position of the aluminum foil fixed in the reaction solution is a key point in controlling the final morphology of the 2D nanostructures. If the foil were placed at the bottom of the solution, the silver nanosheets would be partially covered by spherical nanoparticles that are rather difficult to be removed completely by rinsing or ultrasonic vibration. The

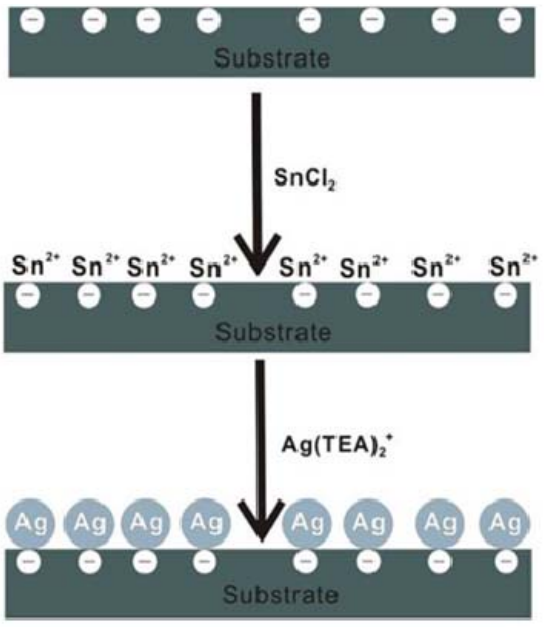

Fig. 6: Schematic illustration of the electroless plating method. Reproduced with permission from ref.35, copyright 2013, Springer.

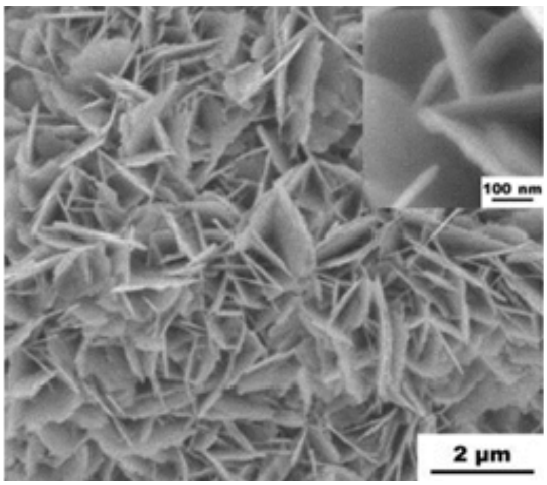

Fig. 7: SEM image of 2D staggered silver nanosheets deposited on an aluminum foil. Reproduced with permission from ref.37, copyright 2005, IOP science.

foil was carefully fixed to make its lower surface in contact with the solution and kept its upper surface outside the solution. This modification can effectively avoid irregular deposition and generate a particle-free 2D nanostructure. The surface property of the aluminum foil can also affect the morphology of the 2D silver nanostructure [37]. Moreover, Xu et al. fabricated polyaniline particles into membranes and films, and it is found that metal nanoparticles like Ag, Au, Pt and Pd can be directly deposited onto those membranes and films. Interestingly, the morphology and size of them can be well controlled by tuning the chemical nature (acid dopant) of the polyaniline membranes and films. Also, it was demonstrated that homogeneous three-dimensional Ag nanostructures produced on Au-supported polyaniline membranes could be promising SERS substrates. Compared to the metal structures fabricated on silicon substrates, Ag nanostructures fabricated onto conducting polymer substrates are much more cost-effective and attractive for SERS applications. Figure 8 shows the Ag structures grown on citric acid doped P–CNTs membranes in $AgNO_3$ aqueous solutions with different concentrations. The prepared well-defined Ag nanosheet hierarchical structures show strong SERS responses toward the analyte molecule, with a detection sensitivity down to 5 ppm [38].

Redox reaction

Another one-step process is synthesis of silver nanosheets by redox reaction. The recently work reported by Chen et al. is about synthesis of nanocables by redox reaction between $AgNO_3$ and pyrrole in the presence of poly(vinylpyrrolidone) [39]. Silver atoms were formed when $AgNO_3$ was added to a pyrrole solution, then they were transformed to silver-PPy nanosheets with regular morphology. Poly(vinylpyrrolidone) (PVP) plays crucial roles in this process: as a capping agent to form silver nanowires, and as a dispersant of pyrrole monomers, which can influence the site at which pyrrole monomer exists. It is believed that PVP can control the growth rates of various faces of silver by coordinating to the surfaces. Ag-C coaxial nanocables have been fabricated under hydrothermal conditions using starch and silver nitrate as starting materials. The morphology and the aspect ratio of silver-PPy nanocables can be controlled by adjusting the molar concentration ratio of pyrrole to $AgNO_3$. Before PVP and AgNO3 were dropped into the flask, the pyrrole

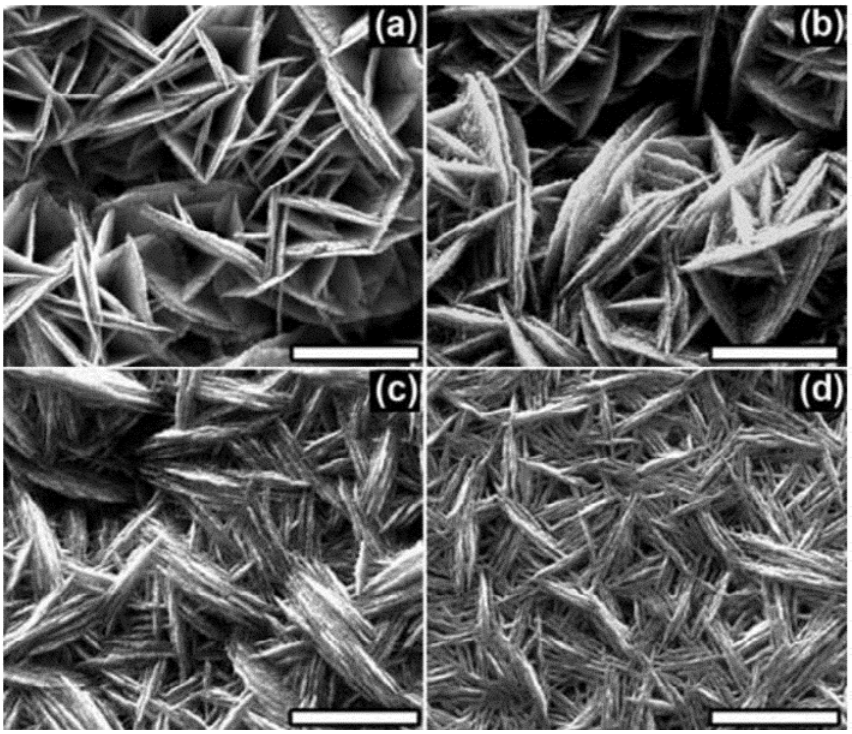

Fig. 8: SEM images of silver nanostructures produced by immersing the P–CNTs membranes doped by citric acid in (a) 15, (b) 25, (c) 50 and (d) 100 mM $AgNO_3$ solution for 30 min, scale bar: 1 µm. Reproduced with permission from ref.38, copyright 2010, Royal society of chemistry.

monomer was transparent. The reaction was very fast, and the system turned a pale grass-green color as soon as PVP and $AgNO_3$ were dropped into the flask simultaneously. As the reaction continued, the small, unstable nanoparticles of silver spontaneously and slowly dissolved into the solution and recrystallized onto the larger particles (Ostwald ripening). As the reaction continued, more silver-PPy nanosheets connected together to form larger silver-PPy congeries [39].

Mirror reaction

In some methods of synthesis of silver nanoparticle, silver mirror reaction is involved. Historically, the silver mirror reaction is still being used as an efficient method for preparing thin film coatings of silver nanoparticles. Modified silver mirror reaction in which silver ammonia ions were reduced to metallic silver by glucose and an inorganic species, aluminum nitrate, was introduced to the system. Thermodynamic calculation demonstrates that the aluminum hydroxide generated in situ from aluminum nitrate plays a key role in the formation of silver nanosheets. This reaction was carried out in water in the absence of any organic surfactant or polymer, which is so-called soft template. In a reported work, flat silicon wafer is used as the substrate and it was set at the bottom of the normal silver mirror reaction solution. The experimental results demonstrated that the products of normal silver mirror reaction were irregular. The result implies that the addition of ammonium nitrate to the silver mirror reaction mixture is a key factor to produce silver nanosheets. Recently, it was reported that some inorganic species such as NaCl, NaBr and NaOH can be utilized to control the structures of silver nanoparticles in the wet chemical reductions of the in situ formed aluminum hydroxide induced the formation of plate-like silver nanoparticles. The method is facile since it requires neither any organic capping-agent, nor any seeding operation of silver salts [40].

Another example is silver mirror reaction on Al substrate. Silver flowerlike nanostructures can grow only on an oxide-free aluminum surface and for this reason electron-beam lithography is proposed to make desired patterns through a layer of poly(methyl methacrylate) (PMMA), deposited on an Al substrate. The silver mirror reaction is then applied, which results in covering the predefined exposed Al areas with silver nanosheet

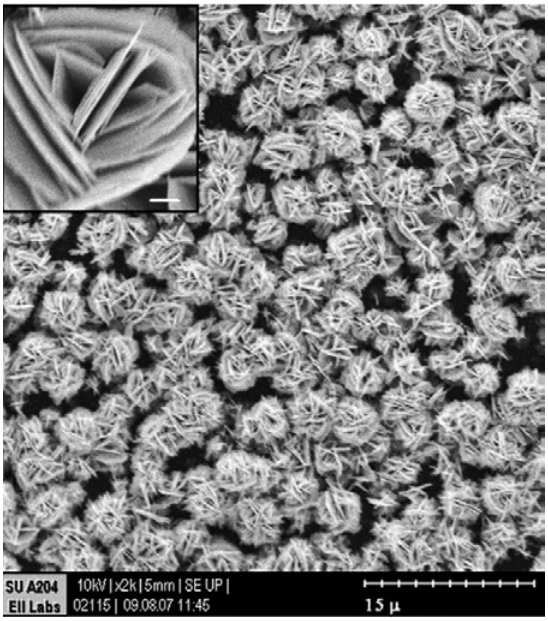

Fig. 9: Silver flowerlike nanostructures grown on a flat Al substrate. Reproduced with permission from ref.41, copyright 2008, Elsevier.

structures. The morphology of the Ag flowers showed no dependence that whether a foil or a thin Al layer is used. An exemplary electron microscopy photograph of silver nanostructures grown on Al layer on glass is shown on Figure 9 [41]. Another way to synthesis silver nanoparticle involving silver mirror reaction is silver mirror reaction on copper foil. Silver nanoclusters with various morphologies ranging from the leaflike to flowerlike hierarchical structures can be produced from the silver mirror reaction on commercially available copper foils after being treated with a dilute aqueous HCl solution under different conditions. However, when the silver mirror reaction was performed on a commercially available copper foil (Figure 10a) under the same conditions, large scale leaf-like microstructures of a fractal geometry were formed (Figure 10b,c). SEM images taken under a higher magnification (Figure 10d,e) clearly show that these "leaves" are composed of a large number of polygonal nanosheets with a thickness of about 200 nm self-assembled into a 3D hierarchical structure. The EDX analyses on the cluster "building blocks" (Figure 10f) clearly show a major peak of silver with a much weaker peak for Cu, arising from the copper substrate. The surface morphology and chemical state of Cu foils play important roles in regulating the structure features, and hence properties, of the resulting silver cluster [42].

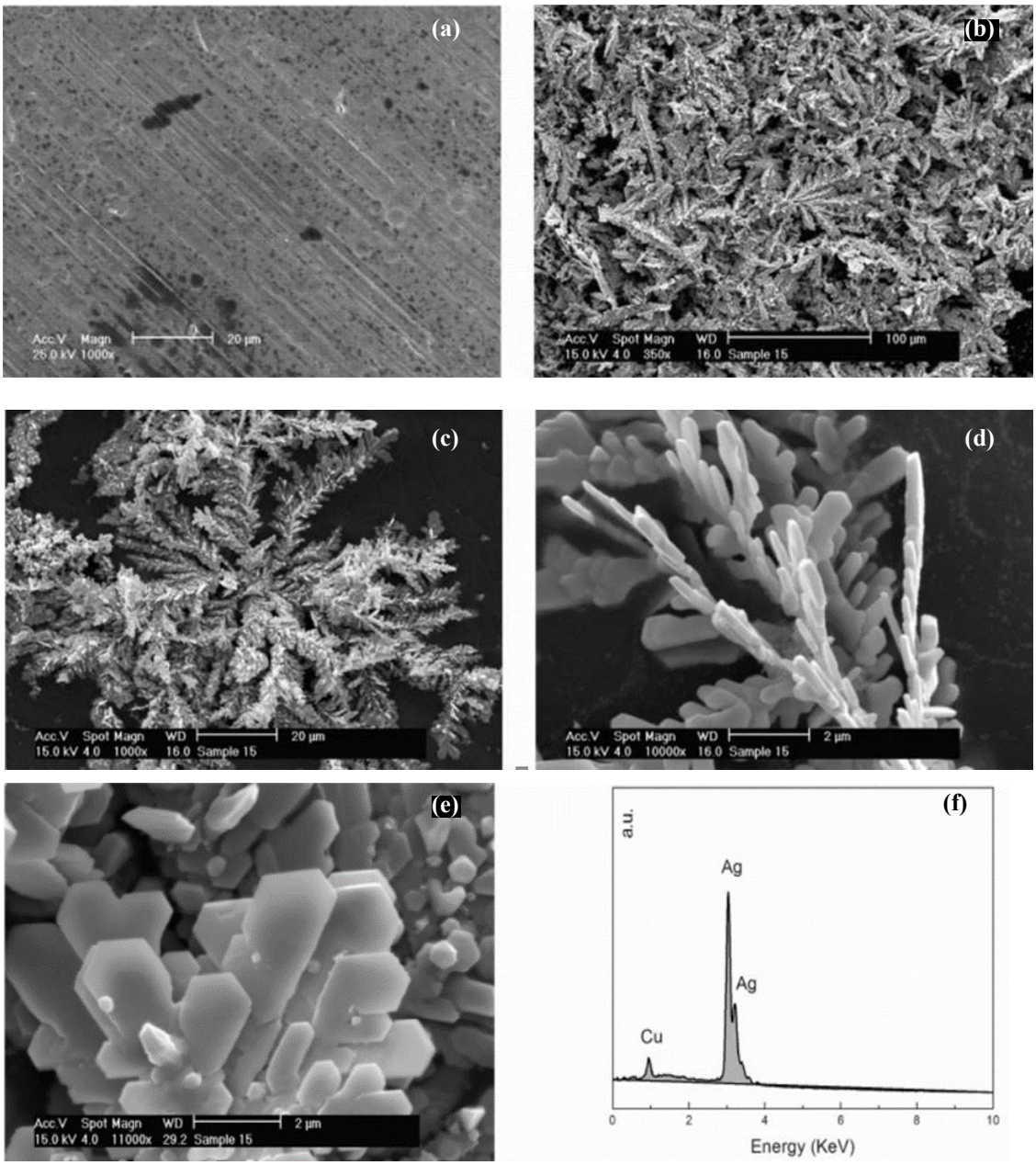

Fig. 10: SEM images of (a) surface of the Cu foil, (b,c) leaflike silver microstructures formed on the Cu surface, (d,e) as for (c) taken from different areas under a higher magnification, and (f) EDX spectrum of the silver nanoclusters. Reproduced with permission from ref.42, copyright 2005, American Chemical Society

Also fabricate silver– polypyrrole (Ag–PPy) composite by the modified silver mirror reaction is reported by Wang et al. [36]. The small size, large surface area, and plate-like structure of the silver nanosheets were deposited on the surface of PPy. The obtained Ag–PPy substrate is very stable, inexpensive, and exhibits excellent SERS enhancement ability. The as-prepared silver–PPy composites exhibit excellent enhancement ability as SERS substrate, which are expected to have wide applications in sensor and another related field [43].

Coating technique

A coating technique also is used to make sintered Ag nanosheets. If thermal reduction of the silver precursor after coating is carefully optimized, good sintered silver nanosheets can

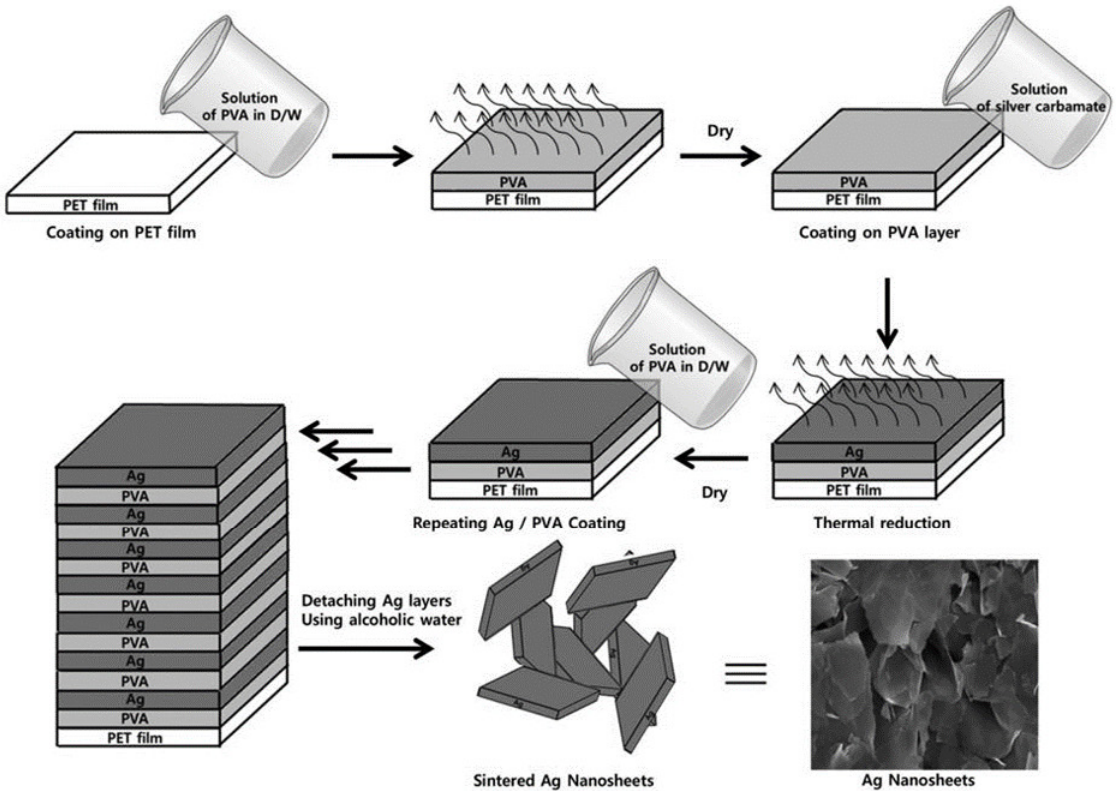

Fig. 11: Schematic procedures for preparation of sintered Ag nanosheets using coating process. Reproduced with permission from ref.19, copyright 2015, Elsevier.

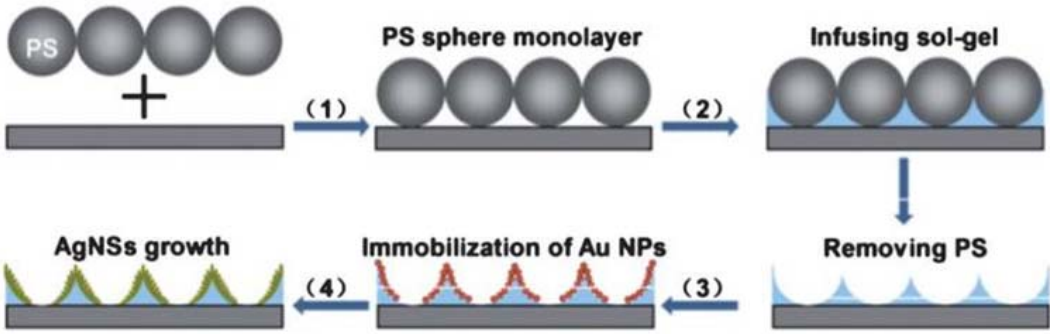

Fig. 12: A schematic illustration of the fabrication process of a 2D Ag nanosheet coated inverse opal film. Reproduced with permission from ref.45, copyright 2012, Royal Society of Chemistry.

be obtained from a silver film using coating technologies after removing sacrificial materials. This process uses coated thin layers of PVA and silver 2-ethylhexylcarbamate (AgEHC), followed by thermal reduction. The PVA layer could easily dissolve away from the multi-layers of PVA/Ag; thus, residual sintered silver nanosheets were separated from an alcoholic solution via sonication for several minutes. Fig. 11 shows the overall fabrication scheme. Wire-bar coating using PVA and Ag-EHC solutions was employed to separate the PVA and silver layers, respectively [19].

Self -seeding or self-assembling process

Silver nanosheets also can be synthesized by self-seeding. For example, Ag nanosheets were fabricated by self-seeding through a facile binary reductant strategy run in the aqueous solution of

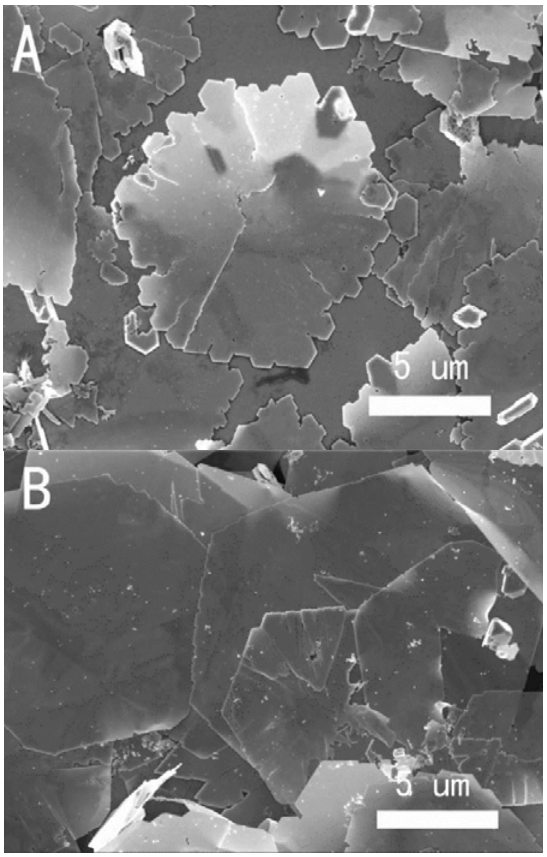

Fig. 13: Typical SEM images of the Ag nanosheets using 10 µL (A) and 100 µL (B) of H_2O_2. Reproduced with permission from ref.46, copyright 2010, American Chemical Society.

PVP–SDS aggregations. A trace amount of $NaBH_4$ was added into the early phase to generate tiny Ag nanocrystals that were used as the seeds for the subsequent growth of Ag nanoplates, in which PVP served as a mild reducing agent and as the supplement of $NaBH_4$. The size and morphology of the nanosheets could be gently regulated with the concentrations of PVP or SDS and the pH of the reaction solution, while the dramatic variance of size and morphology was primarily induced by $NaBH_4$ concentration. Free PVP monomers with lower concentration induced irregular particles, while the lower concentration of $NaBH_4$ led to the formation of small and regular nanosheets. Both particle size and morphology could be regulated with SDS concentration. If the SDS concentration was higher than the critical aggregation concentration, higher SDS concentrations favored smaller particle sizes and nanosheet formation. PVP is a well-known non-ionic polymeric template for nanoparticle synthesis, and PVP–SDS can self-assemble into aggregations with significant surface ordering, therefore, it could serve as a template or microreactor to generate various morphologies of nanoparticles [44].

He et al. reported a two dimensional (2D) macroporous Ag film composed of a silver nanosheet (AgNS)-coated inverse opal film which is easily prepared by a self-assembly method without the requirement of special equipment and treatment [45]. The prepared AgNS-coated films are highly active SERS substrates, yielding an enhancement factor of 6×10^7 and reproducible SERS signals. The fabrication procedure of the 2D AgNS-coated inverse opal film is schematically illustrated in Figure 12. Briefly, PS microspheres were self-assembled into monolayers (step 1). The ordered inverse opal film was then prepared by using the monolayer as a template (step 2). Afterwards, AuNPs were immobilized on the film surface (step 3). AgNSs are finally grown on the inverse opal film via a simple chemical reaction (step 4). The PS microspheres with a diameter of ~510 nm are self-assembled into a closely packed monolayer on the surface of a silicon wafer, which acts as a template for the fabrication of the inverse opal film [45].

Wet chemical method

Silver nanosheets can be also fabricated without using any seed, polymers, surfactants or sacrificial substrates. Through the addition of a small quantity of H_2PdCl_4, Chen et al. demonstrated that $AgNO_3$ can be easily reduced by H_2O_2 in basic aqueous solution at room temperature and under normal pressure [46]. It is found that H_2PdCl_4 plays a vital role in forming the micrometer-size silver nanosheets. This work has some advantages such as: (i) It is a facile and environmentally friendly method conducted at room temperature and under normal pressure without using any seeds or sacrificial substrates, (ii) The absence of a reaction solution of organic long-alkyl-chain surfactants or polymers provides a relatively "clean" environment to grow silver nanosheets, (iii) The edge lengths of the silver nanosheets obtained may reach 10-15 µm in size with potential applications as SERS, electrochemical SPR, or STM substrates [46]. The influence of H_2O_2 on the morphology of the Ag nanosheets was investigated. As seen in Figure 13, the morphology of the Ag nanosheets formed was not changed significantly when the quantity of the H_2O_2 was reduced from 50 to 10 µL or increased

to 100 µL. The only larger difference between these samples is that the Ag nanosheets obtained at 100 µL of H_2O_2 have more smooth edges than those obtained at 10 µL of H_2O_2.

CONCLUSIONS

The present investigation is focused on the synthesis of two dimensional silver(I) coordination polymer, [Ag(µ5-T4S)]n (1), which can be used as new precursor for preparation of silver and silver sulfate nanostructures by calcination process. Calcination process of 1 was performed at 450, 500 and 700 °C in a furnace and static atmosphere of air. XRD pattern of the residue obtained from calcination of 1 at 450 °C is different from those obtained from calcination of it at 500 and 700 °C. With attention to the TG analysis, we find out that calcination of 1 is not complete at 450 °C and we could not identify the product formed by calcination of it at this temperature. At 500 °C, the final residue product is formed. Thus, the resulting compounds from calcination of 1 at 500 and 700 °C are compacted mixtures of silver and silver sulfate nanosheets and microstructures, respectively. By increasing the temperature from 500 to 700 °C, the tendency of silver and silver sulfate nanosheets to agglomeration was increased. Thus, the appropriate temperature for preparation silver and silver sulfate nanosheets from 1 is 500 °C. Furthermore different methods of synthesizing silver nanosheets were reviewed in this paper. In addition to calcination process reported by us, here other procedures such as electrochemical deposition methods, electro less deposition method, direct deposition method, redox reaction, mirror reaction, coating technique, self-seeding or self-assembling process and wet chemical method employed so far for the synthesis of silver nanosheets were also reviewed.

ACKNOWLEDGEMENTS

The authors would like to acknowledge the financial support of University of Tehran for this research under grant number 01/1/389845.

CONFLICT OF INTEREST

The authors declare that there is no conflict of interests regarding the publication of this manuscript.

REFERENCES

1. Fardood ST, Ramazani A, Moradi S. Green synthesis of Ni–Cu–Mg ferrite nanoparticles using tragacanth gum and their use as an efficient catalyst for the synthesis of polyhydroquinoline derivatives. Journal of Sol-Gel Science and Technology. 2017;82(2):432-9.
2. Tarasi R, Khoobi M, Niknejad H, Ramazani A, Ma'mani L, Bahadorikhalili S, et al. β -cyclodextrin functionalized poly (5-amidoisophthalicacid) grafted Fe 3 O 4 magnetic nanoparticles: A novel biocompatible nanocomposite for targeted docetaxel delivery. Journal of Magnetism and Magnetic Materials. 2016;417:451-9.
3. Dayyani N, Khoee S, Ramazani A. Design and synthesis of pH-sensitive polyamino-ester magneto-dendrimers: Surface functional groups effect on viability of human prostate carcinoma cell lines DU145. European Journal of Medicinal Chemistry. 2015;98:190-202.
4. Fardood ST, Atrak K, Ramazani A. Green synthesis using tragacanth gum and characterization of Ni–Cu–Zn ferrite nanoparticles as a magnetically separable photocatalyst for organic dyes degradation from aqueous solution under visible light. Journal of Materials Science: Materials in Electronics. 2017;28(14):10739-46.
5. Aghahosseini H, Ramazani A, Ślepokura K, Lis T. The first protection-free synthesis of magnetic bifunctional l -proline as a highly active and versatile artificial enzyme: Synthesis of imidazole derivatives. Journal of Colloid and Interface Science. 2018;511:222-32.
6. Motevalizadeh SF, Khoobi M, Sadighi A, Khalilvand-Sedagheh M, Pazhouhandeh M, Ramazani A, et al. Lipase immobilization onto polyethylenimine coated magnetic nanoparticles assisted by divalent metal chelated ions. Journal of Molecular Catalysis B: Enzymatic. 2015;120:75-83.
7. Kitagawa S, Kitaura R, Noro S-i. Functional Porous Coordination Polymers. Angewandte Chemie International Edition. 2004;43(18):2334-75.
8. Akhbari K, Morsali A. Modulating methane storage in anionic nano-porous MOF materials via post-synthetic cation exchange process. Dalton Transactions. 2013;42(14):4786.
9. Batten SR, Murray KS. Structure and magnetism of coordination polymers containing dicyanamide and tricyanomethanide. Coordination Chemistry Reviews. 2003;246(1-2):103-30.
10. Akhbari K, Morsali A. Silver nanofibers from the nanorods of one-dimensional organometallic coordination polymers. CrystEngComm. 2010;12(11):3394.
11. Akhbari K, Hemmati M, Morsali A. Fabrication of Silver Nanoparticles and 3D Interpenetrated Coordination Polymer Nanorods from the Same Initial Reagents. Journal of Inorganic and Organometallic Polymers and Materials. 2010;21(2):352-9.
12. Bashiri R, Akhbari K, Morsali A, Zeller M. A three-dimensional AgI coordination polymer constructed via η2 Ag–C bonds: Thermal, fluorescence, structural and solution studies. Journal of Organometallic Chemistry. 2008;693(10):1903-11.
13. Akhbari K, Morsali A, Rafiei S, Zeller M. A new two-dimensional AgI coordination polymer with Ag C interactions: Thermal, fluorescence, structural and solution studies. Journal of Organometallic Chemistry. 2008;693(2):257-62.
14. Akhbari K, Morsali A, Zeller M. Unique Ag–C bonds, thermal, fluorescence, structural and solution studies of two-dimensional silver(I) coordination polymer. Journal of Organometallic Chemistry. 2007;692(17):3788-95.
15. Griffith EAH, Amma EL. Metal ion-aromatic complexes. XVIII. Preparation and molecular structure of naphthalenetetrakis(silver perchlorate) tetrahydrate. Journal

of the American Chemical Society. 1974;96(3):743-9.
16. Ning GL, Wu LP, Sugimoto K, Munakata M, Kuroda-Sowa T, Maekawa M. Construction of 2-D multilayer structures: silver(I) complexes with linear aromatic compounds. Journal of the Chemical Society, Dalton Transactions. 1999(15):2529-36.
17. Munakata M, Wu LP, Kuroda-Sowa T, Maekawa M, Suenaga Y, Ning GL, et al. Supramolecular Silver(I) Complexes with Highly Strained Polycyclic Aromatic Compounds. Journal of the American Chemical Society. 1998;120(34):8610-8.
18. Wang R. Nanoparticles: from theory to application: G nter Schmid (ed), WILEY-VCH Verlag GmbH & Co. KGaA, Weinheim, ISBN 3-527-30507-6, Hbk, 444 pages, price 159,00 Euro. Colloid and Polymer Science. 2004;283(4):466-.
19. Ahn H-Y, Cha J-R, Gong M-S. Preparation of sintered silver nanosheets by coating technique using silver carbamate complex. Materials Chemistry and Physics. 2015;153:390-5.
20. Biswas A, Aktas OC, Schürmann U, Saeed U, Zaporojtchenko V, Faupel F, et al. Tunable multiple plasmon resonance wavelengths response from multicomponent polymer-metal nanocomposite systems. Applied Physics Letters. 2004;84(14):2655-7.
21. Stegeman GI, Wright EM. All-optical waveguide switching. Optical and Quantum Electronics. 1990;22(2):95-122.
22. Wei H, Eilers H. From silver nanoparticles to thin films: Evolution of microstructure and electrical conduction on glass substrates. Journal of Physics and Chemistry of Solids. 2009;70(2):459-65.
23. Talley CE, Jackson JB, Oubre C, Grady NK, Hollars CW, Lane SM, et al. Surface-Enhanced Raman Scattering from Individual Au Nanoparticles and Nanoparticle Dimer Substrates. Nano Letters. 2005;5(8):1569-74.
24. Braun G, Pavel I, Morrill AR, Seferos DS, Bazan GC, Reich NO, et al. Chemically Patterned Microspheres for Controlled Nanoparticle Assembly in the Construction of SERS Hot Spots. Journal of the American Chemical Society. 2007;129(25):7760-1.
25. Shegai T, Li Z, Dadosh T, Zhang Z, Xu H, Haran G. Managing light polarization via plasmon-molecule interactions within an asymmetric metal nanoparticle trimer. Proceedings of the National Academy of Sciences. 2008;105(43):16448-53.
26. Iwantono, Taer E, Umar AA, Saputrina TT. Synthesis of silver nanosheets onto solid substrates by using seed-mediated growth method. AIP; 2013. p. 79-82.
27. Akhbari K, Morsali A. Preparation of a Three-Dimensional Silver(I) Nano-Coordination Polymer from its Single Crystals by Thermal Treatment with Oleic Acid. Zeitschrift für anorganische und allgemeine Chemie. 2012;638(3-4):692-7.
28. Akhbari K, Morsali A. Preparation of silver nanoparticles from silver(I) nano-coordination polymer. Inorganica Chimica Acta. 2010;363(7):1435-40.
29. Hojaghani S, Akhbari K, Sadr MH, Morsali A. Sonochemical syntheses of one-dimensional silver(I) supramolecular polymer: A precursor for preparation of silver nanostructure. Inorganic Chemistry Communications. 2014;44:1-5.
30. Akhbari K, Morsali A, Retailleau P. Silver nanoparticles from the thermal decomposition of a two-dimensional nano-coordination polymer. Polyhedron. 2010;29(18):3304-9.
31. Akhbari K, Morsali A. Solid-State Structural Transformations of Two AgI Supramolecular Polymorphs to Another Polymer upon Absorption of HNO3 Vapors. Inorganic Chemistry. 2013;52(6):2787-9.
32. Bashiri R, Akhbari K, Morsali A. Nanopowders of 3D AgI coordination polymer: A new precursor for preparation of silver nanoparticles. Inorganica Chimica Acta. 2009;362(4):1035-41.
33. Xia Y, Wu Y, Hang T, Chang J, Li M. Electrodeposition of High Density Silver Nanosheets with Controllable Morphologies Served as Effective and Reproducible SERS Substrates. Langmuir. 2016;32(14):3385-92.
34. Park SH, Son JG, Lee TG, Park HM, Song JY. One-step large-scale synthesis of micrometer-sized silver nanosheets by a template-free electrochemical method. Nanoscale Research Letters. 2013;8(1):248.
35. Yi Z, Xu X, Fang Q, Wang Y, Li X, Tan X, et al. Fabrication of silver nanosheets on quartz glass substrates through electroless plating approach. Applied Physics A. 2013;114(2):485-93.
36. Zhao J, Lin J, Li X, Zhao G, Zhang W. Silver nanoparticles deposited inverse opal film as a highly active and uniform SERS substrate. Applied Surface Science. 2015;347:514-9.
37. He Y, Wu X, Lu G, Shi G. Fabrication of two-dimensional staggered silver nanosheets on an aluminium foil. Nanotechnology. 2005;16(6):791-6.
38. Xu P, Zhang B, Mack NH, Doorn SK, Han X, Wang H-L. Synthesis of homogeneous silver nanosheet assemblies for surface enhanced Raman scattering applications. Journal of Materials Chemistry. 2010;20(34):7222.
39. Chen A, Kamata K, Nakagawa M, Iyoda T, Haiqiao, Li X. Formation Process of Silver−Polypyrrole Coaxial Nanocables Synthesized by Redox Reaction between AgNO3and Pyrrole in the Presence of Poly(vinylpyrrolidone). The Journal of Physical Chemistry B. 2005;109(39):18283-8.
40. He Y, Wu X, Lu G, Shi G. A facile route to silver nanosheets. Materials Chemistry and Physics. 2006;98(1):178-82.
41. Tsutsumanova G, Lyutov L, Tzonev A, Russev S. Ordering of silver flowerlike nanosheet structures on an aluminium substrate. Materials Letters. 2008;62(20):3588-90.
42. Qu L, Dai L. Novel Silver Nanostructures from Silver Mirror Reaction on Reactive Substrates. The Journal of Physical Chemistry B. 2005;109(29):13985-90.
43. Wang W, Zhang R. Silver–polypyrrole composites: Facile preparation and application in surface-enhanced Raman spectroscopy. Synthetic Metals. 2009;159(13):1332-5.
44. Fan Y, Ren Y, Wu M, Fang Y. Self-seeding synthesis of silver nanosheets with binary reduction in poly(vinylpyrrolidone)–sodium dodecyl sulphate aggregation microreactor. Micro & Nano Letters. 2014;9(10):726-30.
45. He L, Huang J, Xu T, Chen L, Zhang K, Han S, et al. Silver nanosheet-coated inverse opal film as a highly active and uniform SERS substrate. J Mater Chem. 2012;22(4):1370-4.
46. Chen H, Simon F, Eychmüller A. Large-Scale Synthesis of Micrometer-Sized Silver Nanosheets. The Journal of Physical Chemistry C. 2010;114(10):4495-501.